



Providing Choice & Value

Generic CT and MRI Contrast Agents



**FRESENIUS
KABI**

CONTACT REP

AJNR

**Role of Apparent Diffusion Coefficient Values
in Differentiation Between Malignant and
Benign Solitary Thyroid Nodules**

A.A.K. Abdel Razek, A.G. Sadek, O.R. Kombar, T.E.
Elmahdy and N. Nada

This information is current as
of July 29, 2025.

AJNR Am J Neuroradiol 2008, 29 (3) 563-568

doi: <https://doi.org/10.3174/ajnr.A0849>

<http://www.ajnr.org/content/29/3/563>

ORIGINAL
RESEARCH

A.A.K. Abdel Razek
A.G. Sadek
O.R. Kombar
T.E. Elmahdy
N. Nada

Role of Apparent Diffusion Coefficient Values in Differentiation Between Malignant and Benign Solitary Thyroid Nodules

BACKGROUND AND PURPOSE: Accurate imaging characterization of a solitary thyroid nodule has been clearly problematic. The purpose of this study was to evaluate the role of the apparent diffusion coefficient (ADC) values in the differentiation between malignant and benign solitary thyroid nodules.

MATERIALS AND METHODS: A prospective study was conducted in 67 consecutive patients with solitary thyroid nodules who underwent diffusion MR imaging of the thyroid gland. Diffusion-weighted MR images were acquired with b factors of 0, 250, and 500 s/mm² by using single-shot echo-planar imaging. ADC maps were reconstructed. The ADC values of the solitary thyroid nodules were calculated and correlated with the results of histopathologic examination. Statistical analysis was performed.

RESULTS: The mean ADC value of malignant solitary thyroid nodules was $0.73 \pm 0.19 \times 10^{-3}$ mm²/s and of benign nodules was $1.8 \pm 0.27 \times 10^{-3}$ mm²/s. The mean ADC values of malignant nodules were significantly lower than those of benign ones ($P = .0001$). There were no significant differences between the mean ADC values of various malignant thyroid nodules, but there were significant differences between the subtypes of benign thyroid nodules ($P = .0001$). An ADC value of 0.98×10^{-3} mm²/s was proved as a cutoff value differentiating between benign and malignant nodules, with 97.5%, 91.7%, and 98.9% sensitivity, specificity, and accuracy, respectively.

CONCLUSION: The ADC value is a new promising noninvasive imaging approach used for differentiating malignant from benign solitary thyroid nodules.

Nodular thyroid is commonly detected on palpation in 4%–7% of the population,^{1,2} on sonographic examination in 10%–40%, and by pathologic examination at autopsy in 50%.^{3,4} In contrast, compared with the high prevalence of nodular thyroid disease, thyroid cancer is rare. The challenge of imaging thyroid nodules is to reassure most patients who have benign disease and to diagnose the minority of patients who will prove to have a malignancy.^{5,6}

Ultrasonography has been used in the assessment of the thyroid nodules as a primary imaging technique.^{2,7,8} Currently, there is no single sonographic criterion that can reliably distinguish benign from malignant thyroid nodules.^{4,9} The results of predicting thyroid cancer with color Doppler sonography are controversial, with some reporting that Doppler sonography is helpful and others reporting that it did not improve diagnostic accuracy.^{4,5,10,11} The hazards of radiation exposure are unavoidable in nuclear scintigraphy,² and not all functioning nodules on scintigraphy are benign.^{6,9} The risk of cancer in a cold nodule is 4 times more common than in a hot nodule.^{3,6} Fine-needle aspiration biopsy (FNAB) with cytologic evaluation is commonly used, but it is inconclusive in 15%–20% of patients, in addition to the possible, but less likely, associated hemorrhage.^{2,4} The incidence of cancer in patients with thyroid nodules selected for FNAB is approximately 9.2%–13%.⁵ FNAB is considered an effective method for differentiating between benign and malignant thyroid nodules.^{4,7,12–14}

Routine T1- and T2-weighted MR imaging has a limited role

in the evaluation of thyroid nodules. It cannot distinguish benign from malignant nodules or assess the functional status of thyroid nodules.^{12–15} Diffusion-weighted MR imaging has been used to characterize head and neck tumors, in which there are significant differences in the apparent diffusion coefficient (ADC) values of malignant tumors and benign lesions.^{16–19} Tezuka et al,²⁰ in their study using diffusion-weighted MR imaging to assess the thyroid function, reported that the ADC values of patients with Grave's disease exceeded those of patients with subacute thyroiditis, with a sensitivity and specificity of 75% and 80%, respectively, in differentiating between both disease entities. They concluded that diffusion-weighted MR imaging could be clinically important in evaluating the thyroid function. To our knowledge, there have been no articles about diffusion-weighted MR imaging evaluating thyroid nodules.

The aim of our study was to evaluate the role of ADC values in differentiating between malignant and benign solitary thyroid nodules.

Methods

A prospective study was conducted in 67 consecutive patients (48 women, 19 men; 20–72 years of age; mean, 47 years of age) with sonographically diagnosed solitary thyroid nodules, who were candidates for surgery. Both solid and cystic solitary thyroid nodules were included in this study. Four patients were excluded from the study due to motion artifacts in 2 patients and bad image quality in another 2 patients. Sixty-three patients were finally selected. We obtained institutional review board approval from our hospital and informed consent from the patients before the study. All patients were subjected to clinical and MR imaging examinations of the thyroid gland.

The MR imaging studies were performed with a 1.5T MR imaging system (Symphony; Siemens, Erlangen, Germany) by using a neck circular polarization surface coil. The neck array coil was carefully placed so that the thyroid gland would be located in the central part of the FOV in

Received June 16, 2007; accepted after revision August 22.

From the Departments of Diagnostic Radiology (A.A.K.A.R., A.G.S., O.R.K.), Endocrine Surgery (T.E.E.), and Pathology (N.N.), Mansoura Faculty of Medicine, Mansoura, Egypt.

Please address correspondence to Ahmed Abdel Khalek Abdel Razek, MD, Diagnostic Radiology Department, Mansoura Faculty of Medicine, 62 El Nokrasi St, Mansoura, Egypt; e-mail: arazek@mans.eun.eg

DOI 10.3174/ajnr.A0849

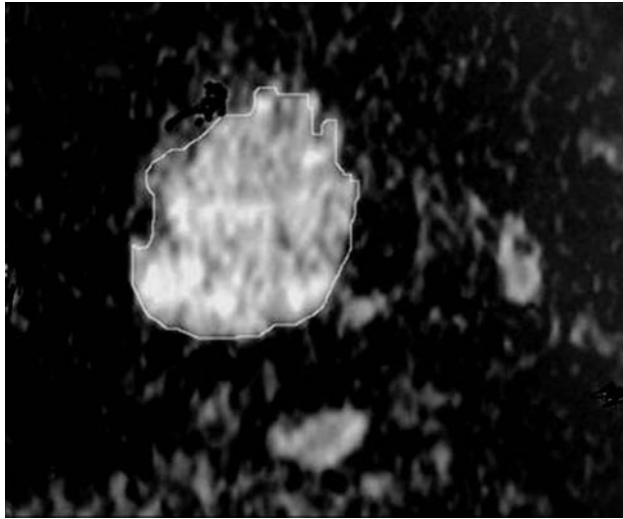


Fig 1. Measurement of the ADC value of a thyroid nodule in an ADC map image. The region of interest is drawn around the thyroid nodule, and the ADC value is measured.

each subject. The magnet is equipped with a self-shielded gradient set for echo-planar imaging. All patients underwent conventional T1- (TR/TE, 500/15 ms) and T2-weighted MR imaging (TR/TE, 6000/80 ms) with a section thickness of 4 mm, an intersection gap of 1 mm, FOV of 20–25 cm, and an acquisition matrix of 256×224 . Images were obtained in the axial and coronal planes, after scout sagittal ones.

Diffusion-weighted MR images were obtained by using a multisection single-shot echo-planar imaging sequence. A set of multiple axial scans of the neck was obtained to cover the thyroid gland. Imaging parameters were the following: TR = 10,000 ms, TE = 108 ms, NEX = 1, bandwidth = 125 kHz, matrix of 256×128 , FOV of 20–25 cm, section thickness of 4 mm, and intersection gap of 1 mm. The diffusion gradients were applied in 3 orthogonal directions (X, Y, and Z). The pixel size was 2.3×2.3 mm. Fat suppression was added to the diffusion-weighted imaging by placing the frequency-selective radio-frequency pulse before the pulse sequence to avoid severe chemical-shift artifacts. Diffusion-weighted MR images were acquired with diffusion factors (b factor) of 0, 250, and 500 s/mm^2 , and the ADC maps were then reconstructed. Diffusion-weighted MR scanning time was <2 minutes.

The 3 radiologists sharing in the study determined by consensus whether the ADC maps were acceptable for further analysis. Special attention was paid to image distortion by susceptibility artifacts. A quantitative analysis of the diffusion-weighted MR images was made. All images were interpreted by 1 radiologist specializing in head and neck imaging. The region of interest was drawn by 1 radiologist by electronic cursor around the thyroid nodules in the ADC map, and the ADC value was measured, as shown in Fig 1. In case of thyroid nodules with mixed solid and cystic components, the region of interest surrounded the solid portion to avoid the cystic part if possible because it could give a falsely elevated ADC value. The region of interest was placed around the cystic area in patients with thyroid cysts. Discrimination between the cystic and solid nodules was guided by sonographic examination.

The final diagnosis of the solitary thyroid nodule was made by biopsy during surgery for all patients, without knowledge of the ADC values. Biopsy was performed after MR imaging with a time delay of between 7 and 13 days. The histopathologic specimens were interpreted by a pathologist experienced in the head and neck. The histopathologic results were correlated with the ADC values.

Statistical analysis was done by using the Statistical Package for the

Table 1: The ADC values of solitary thyroid nodules in 63 patients

Type of Thyroid Nodules	No. (%) of		Mean ADC Values (mm^2/s)
	Thyroid Nodules	Range of ADC Values (mm^2/s)	
Benign	56 (88.9)	$0.5\text{--}2.3 \times 10^{-3}$	$1.8 \pm 0.27 \times 10^{-3}$
Adenomatous nodule	42 (66.7)	$1.1\text{--}1.9 \times 10^{-3}$	$1.8 \pm 0.14 \times 10^{-3}$
Follicular adenoma	6 (9.5)	$1.2\text{--}2 \times 10^{-3}$	$1.7 \pm 0.17 \times 10^{-3}$
Thyroid cyst	8 (12.7)	$0.5\text{--}2.3 \times 10^{-3}$	$1.9 \pm 0.38 \times 10^{-3}$
Malignant	7 (11.1)	$0.5\text{--}1.1 \times 10^{-3}$	$0.73 \pm 0.19 \times 10^{-3}$
Papillary carcinoma	4 (6.3)	$0.5\text{--}1.1 \times 10^{-3}$	$0.68 \pm 0.23 \times 10^{-3}$
Follicular carcinoma	3 (4.8)	$0.6\text{--}1 \times 10^{-3}$	$0.77 \pm 0.17 \times 10^{-3}$

Social Sciences for Windows (SPSS, Chicago, Ill) program software package. The Mann-Whitney *U* test was performed to compare the histopathologic and quantitative ADC measurements of benign and malignant thyroid nodules. The Kruskal-Wallis test was used to compare the different subtypes of both benign and malignant groups. A value of $P < .05$ was considered significant. We used a receiver operating characteristic (ROC) curve to determine a cutoff value for differentiating malignant from benign solitary thyroid nodules.

Results

The image quality was good and acceptable for interpretation in the 63 finally examined patients. The size of the thyroid nodules ranged from 0.8 to 4.2 cm (mean, 1.5 cm). They were located in the right thyroid lobe in 47 patients and in the left one in 16 patients. The most common thyroid nodule was benign (88.9%), and most of these benign nodules were adenomatous nodules (66.7%). Sonography detected thyroid cyst in 8 patients (12.7%).

Table 1 illustrates the ADC values of the different histopathologic types of solitary thyroid nodules in this study. The ADC value of the adenomatous nodules ranged from 1.1 to $1.9 \times 10^{-3} \text{ mm}^2/\text{s}$ (Fig 2). Also, the range of the ADC value of the solid part of the follicular adenoma was $1.2\text{--}2 \times 10^{-3} \text{ mm}^2/\text{s}$ (Fig 3). The thyroid cysts (Fig 4) revealed the highest mean ADC value ($1.9 \pm 0.38 \times 10^{-3} \text{ mm}^2/\text{s}$) apart from 1 patient with hemorrhagic cyst (Fig 5), whose ADC value was $0.5 \times 10^{-3} \text{ mm}^2/\text{s}$, simulating malignant lesions. The malignant thyroid nodules showed lower ADC values (Figs 6 and 7). The mean ADC value of papillary carcinoma was $0.68 \pm 0.23 \times 10^{-3} \text{ mm}^2/\text{s}$, and that of follicular carcinoma was $0.77 \pm 0.17 \times 10^{-3} \text{ mm}^2/\text{s}$.

There was a significant difference in ADC values of benign and malignant thyroid nodules: All benign nodules had higher mean ADC values ($1.8 \pm 0.27 \times 10^{-3} \text{ mm}^2/\text{s}$) compared with the malignant ones ($0.73 \pm 0.19 \times 10^{-3} \text{ mm}^2/\text{s}$), despite of the overlap in their ADC values, with $P = .0001$ (Table 2). There were insignificant differences in the ADC values of the various malignant nodules, with $P = .464$, unlike in benign nodules, in which there were significant differences between thyroid cysts and the solid nodules (adenomatous nodules and follicular adenomas), with $P = .0001$ (Table 3).

ROC was done to detect cutoff values differentiating benign from malignant solitary thyroid nodules (Fig 8). The area under the curve measured 97%. As shown from analysis of the curve, an ADC value of $0.98 \times 10^{-3} \text{ mm}^2/\text{s}$ or less could be used as an indicator of malignancy, with a sensitivity of 97.5%, a specificity of 91.7%, and an accuracy of 98.9%.

Discussion

A thyroid nodule is a discrete lesion within the thyroid gland that is distinguishable from the adjacent parenchyma. A study

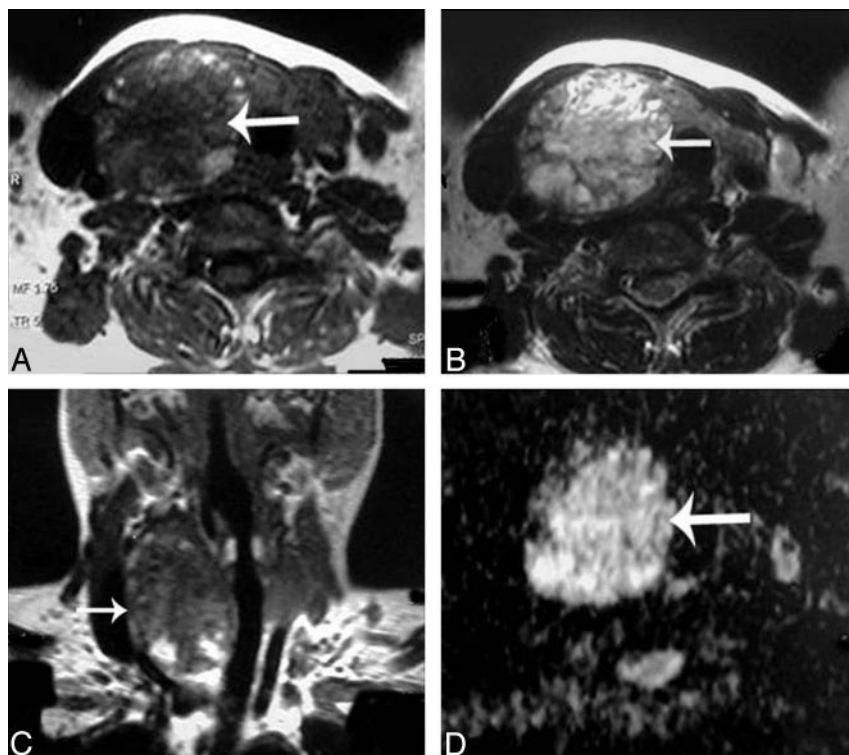


Fig 2. Adenomatous nodule. A–C, Axial T1- and T2-weighted and coronal T1-weighted MR images of the neck, respectively, showing a well-defined oval mainly solid solitary nodule (arrow) affecting the right thyroid lobe with contralateral tracheal displacement. D, An ADC map image with hyperintensity of the nodule (arrow) denoting increased diffusion and a measured ADC value of $1.57 \pm 0.11 \times 10^{-3} \text{ mm}^2/\text{s}$.

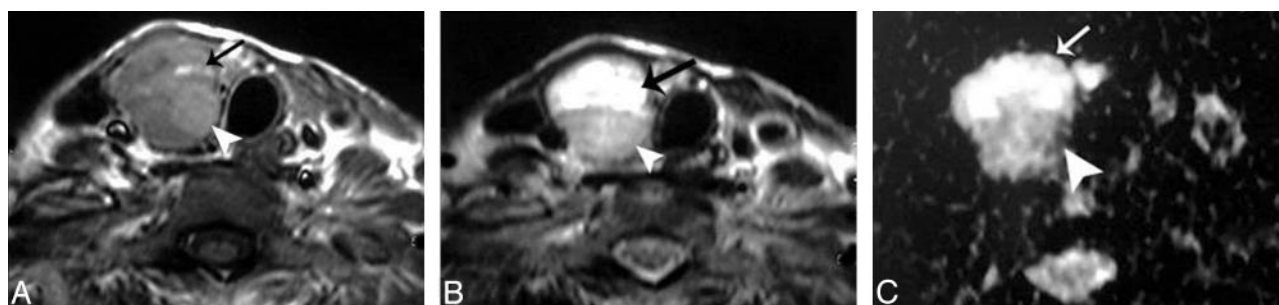


Fig 3. Follicular adenoma. A and B, Axial T1- and T2-weighted MR images, respectively, showing a well-defined more or less oval solitary nodule affecting the right thyroid lobe with contralateral tracheal displacement. The nodule has an anterior cystic part (arrow) and another posterior solid one (arrowhead). C, An ADC map image with marked hyperintensity of the anterior cystic portion of the nodule (arrow), denotes increased diffusion with a measured ADC value of $2.25 \pm 0.18 \times 10^{-3} \text{ mm}^2/\text{s}$ and a relatively hypointense posterior solid portion (arrowhead), denotes relatively restricted diffusion with a measured ADC value of $1.2 \pm 0.08 \times 10^{-3} \text{ mm}^2/\text{s}$.

by sonography of a population group older than 50 years showed that 50% had thyroid nodules.^{4,5} In enlarged nodular thyroids, sonographic examination demonstrated that two thirds had multiple nodules, whereas one third had single nodules. Among these nodules, 85%–90% were proved to be benign.⁴ Most of the benign thyroid nodules were adenomatous nodules (80%), whereas the remaining benign nodules consisted of adenoma, cyst, and focal thyroiditis.^{2,4-6} In the present study, the incidence of benign nodules was 88.9%, and that of malignant ones was 11.1%.

The goal in evaluating a solitary thyroid nodule is to determine whether it is benign or malignant so that patients with thyroid cancer can receive adequate treatment at an earlier stage to reduce possible mortality and morbidity of the disease, while avoiding unnecessary surgery in patients with benign nodules.⁵ It is estimated that surgical excision is decided in approximately 18% of patients who have FNAB on the basis of positive, suspected, or nondiagnostic results and that most of these nodules are benign. It is estimated that only 15%–32%

of patients have cancer. Therefore, most patients who come to surgery for thyroid nodule excision will have an operation for a clinically benign thyroid nodule.¹

Diffusion-weighted MR imaging can provide better characterization of the tissues and their physiologic processes because it reflects the random motion of water protons, which is disturbed by intracellular organelles and macromolecules located in the tissues. Thus, the ADC values of the tissues vary according to the physiologic state of the tissue.^{21,22} Diffusion-weighted MR imaging has been used for differentiation between benign and malignant head and neck masses, characterization of the cervical lymph nodes, and discrimination of recurrent or residual tumors from posttreatment changes in the head and neck.¹⁶⁻¹⁹ Tezuka et al,²⁰ in their study using diffusion-weighted MR imaging to assess the thyroid function reported that the thyroid gland is histologically considered to be an isotropic organ because a significant difference in the ADC value was not observed for the different positions within the gland.

To our knowledge, no previous reports in the literature

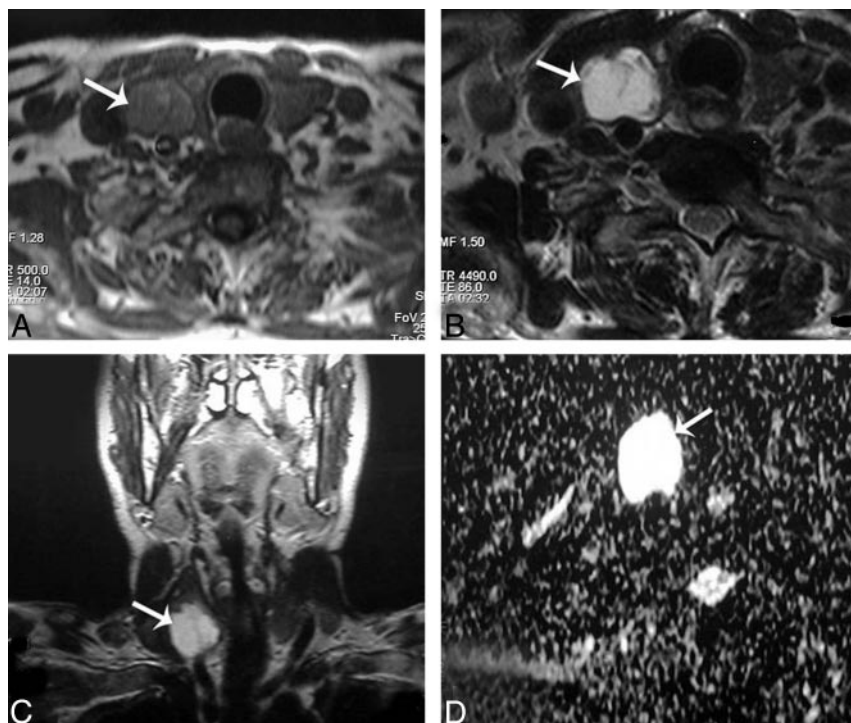


Fig 4. Thyroid cyst. A–C, Axial T1- and T2-weighted and coronal T1-weighted MR images, respectively, showing a well-defined more or less oval solitary nodule (arrow) affecting the right thyroid lobe. D, An ADC map image with marked hyperintensity of the nodule (arrow) denoting increased diffusion, and the measured ADC value is $2.05 \pm 0.13 \times 10^{-3} \text{ mm}^2/\text{s}$.

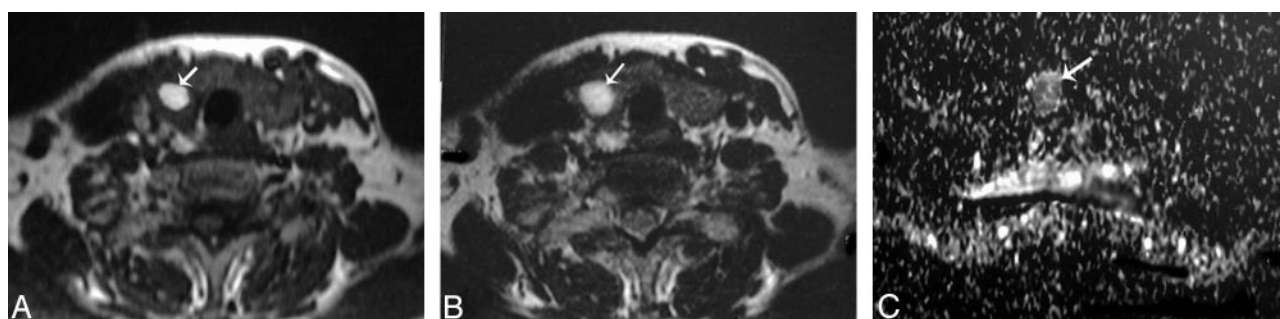


Fig 5. Hemorrhagic thyroid cyst. A and B, Axial T1- and T2-weighted MR images, respectively, showing a small well-defined more or less rounded solitary nodule (arrow) affecting the right thyroid lobe. The nodule is hyperintense on both T1- and T2-weighted images. C, An ADC map image shows low signal intensity of the nodule. The measured ADC value is $0.5 \pm 0.07 \times 10^{-3} \text{ mm}^2/\text{s}$.

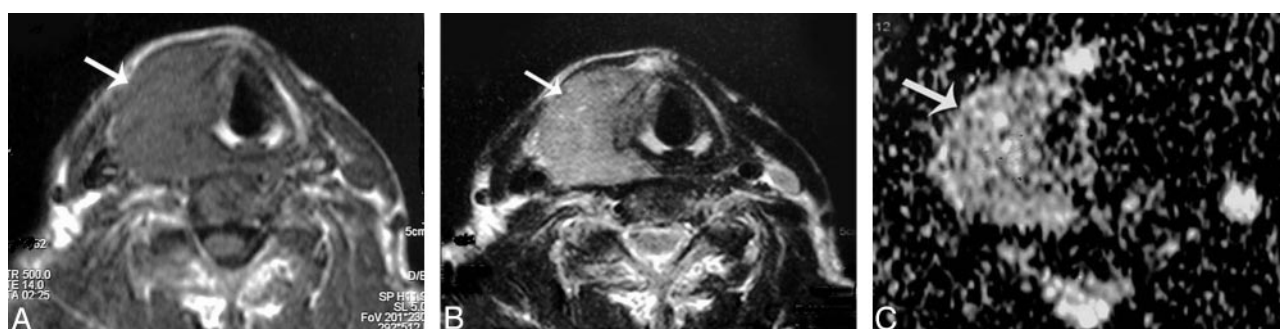


Fig 6. Papillary carcinoma of the thyroid. A and B, Axial T1- and T2-weighted MR images, respectively, showing a well-defined irregular mainly solid solitary nodule (arrow) involving all the right thyroid lobe with contralateral tracheal displacement. C, ADC map image shows hypointensity of the nodule (arrow). The measured ADC value is $0.97 \pm 0.1 \times 10^{-3} \text{ mm}^2/\text{s}$.

described the role of diffusion-weighted MR imaging in the characterization of a solitary thyroid nodule. We evaluated the potential use of diffusion-weighted echo-planar MR imaging in differentiating benign from malignant solitary thyroid nodules and the different subtypes of malignant and benign nodules by determining their ADC values and correlation with the histopathologic results.

The present study showed a significant difference in the ADC values of benign and malignant thyroid nodules, in which all benign nodules had higher mean ADC values compared with the malignant ones, despite the overlap in their ADC values, with $P = .0001$. The difference in the ADC values of thyroid nodules is based on the difference in cellularity and histopathologic features of benign and malignant thyroid



Fig 7. Follicular carcinoma of the thyroid. *A* and *B*, Axial T1- and T2-weighted MR images, respectively, showing a well-defined more or less oval mainly solid solitary nodule (arrowheads) affecting the right thyroid lobe with contralateral tracheal displacement. *C*, ADC map image shows a low ADC value ($0.92 \pm 0.06 \times 10^{-3} \text{ mm}^2/\text{s}$) of the thyroid nodule (arrowhead).

Table 2: Comparison between the ADC values of benign and malignant solitary thyroid nodules

Pathology of Thyroid Nodule	No. (%) of Thyroid Nodules	Mean ADC Values (mm^2/s)	<i>P</i> Value*
Benign	56 (88.9)	$1.8 \pm 0.27 \times 10^{-3}$.0001
Malignant	7 (11.1)	$0.73 \pm 0.19 \times 10^{-3}$	

* Significance was considered when $P < .05$.

Table 3: Comparison between the ADC values in the different subtypes of benign and malignant solitary thyroid nodules

Type of Thyroid Nodule	No. (%) of Thyroid Nodules	Mean ADC Values (mm^2/s)	<i>P</i> Value*
Benign			
Adenomatous nodule	42 (66.7)	$1.8 \pm 0.14 \times 10^{-3}$	
Follicular adenoma	6 (9.5)	$1.7 \pm 0.17 \times 10^{-3}$.0001
Thyroid cyst	8 (12.7)	$1.9 \pm 0.38 \times 10^{-3}$	
Malignant			
Papillary carcinoma	4 (6.3)	$0.68 \pm 0.23 \times 10^{-3}$.464
Follicular carcinoma	3 (4.8)	$0.77 \pm 0.17 \times 10^{-3}$	

* Significance was considered when $P < .05$.

nodules. Cellularity is higher in malignant thyroid nodules compared with benign ones, with reduction of the ADC value. Anderson²³ reported that malignant tumors have enlarged nuclei and hyperchromatism. These histopathologic characteristics reduce the extracellular dimension that results in a decrease in the ADCs of malignant lymph nodes. Preliminary studies that used diffusion-weighted MR imaging in the head and neck have shown good correlation between the ADC values and the histopathologic nature of the tumors.^{16,18} Wang et al¹⁶ reported that the differences in histopathologic features of both benign and malignant head and neck tumors explain the differences in their ADC values. They added that malignant tumors have increased cellularity compared with benign masses, with subsequent decrease of the ADC values.

There is a relatively wide range of ADC values in adenomatous nodules ($1.1\text{--}1.9 \times 10^{-3} \text{ mm}^2/\text{s}$) and follicular adenomas ($1.2\text{--}2 \times 10^{-3} \text{ mm}^2/\text{s}$). This may be explained by the relative abundance of the different components forming these nodules (colloid, microcystic necrosis, hemorrhage, fibrous tissue, and calcification). The contributions of these different components may alter the ADC value and explain the variability of the ADC value found among patients with benign nodules.

Among the thyroid nodules in the present study, 12.7% were found to be cystic. Most thyroid cysts are formed by the degener-

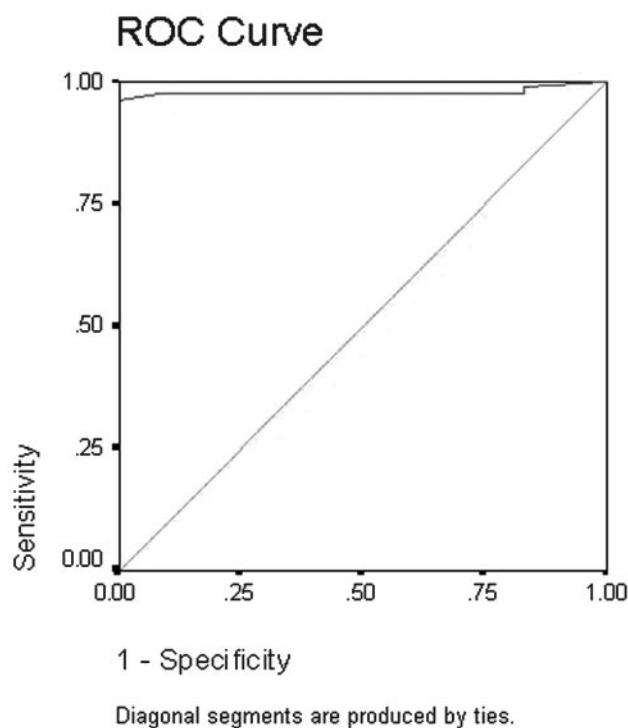


Fig 8. ROC curve of the ADC value used for differentiation of benign from malignant solitary thyroid nodules. The area under the curve measures 97%.

ation of adenomas.^{2,3} A thyroid cyst has the highest ADC value because it may contain serous fluid or may be a colloid cyst with high thyroglobulin concentration. One patient had a hemorrhagic cyst that was misdiagnosed as a malignant tumor with a low ADC value. The cause of this decrease in ADC value was the presence of hemorrhage within the cyst with subsequent restricted diffusion and a low ADC value. There were significant differences between cystic and solid thyroid nodules (adenomatous nodules and follicular adenomas), with $P = .0001$. The cystic or hemorrhagic thyroid nodule did not benefit from diffusion-weighted MR imaging. The FNAB helped in characterization of the nature of the fluid within the thyroid cysts.

In this study, malignant tumors of the thyroid gland showed low ADC values compared with benign nodules, but there were insignificant differences in the mean ADC values of the various malignant nodules, with $P = .464$. Abundant hyperplastic nuclei in malignant tumors and calcified psam-

moma bodies in papillary thyroid carcinoma are responsible for low ADC values. Most thyroid cancers are papillary cancer (75%–80%), whereas the remaining histologic types will consist of approximately 10%–20% follicular, 3%–5% medullary, and 1%–2% anaplastic cancer.¹

In this study, an ADC value of 0.98 is suggestive of a cutoff value differentiating between benign and malignant solitary thyroid nodules, with a sensitivity of 97.5%, a specificity of 91.7%, and an accuracy of 98.9%. Abdel Razek et al¹⁸ reported that when an ADC value of $1.38 \times 10^{-3} \text{ mm}^2/\text{s}$ was used as a threshold value for differentiating malignant from benign cervical lymph nodes, the best results were obtained with an accuracy of 96%, a sensitivity of 98%, and a specificity of 88%. Wang et al¹⁶ reported that a threshold ADC value of $1.22 \times 10^{-3} \text{ mm}^2/\text{s}$ for differentiating benign and malignant tumors of the head and neck has an 86% accuracy, an 84% sensitivity, and a 91% specificity. The results of sonography and color duplex examination in differentiation of benign from malignant thyroid nodules have a sensitivity ranging from 63% to 87%, a specificity from 61% to 95%, and an overall accuracy from 80% to 95%.^{11,12} The FNAB is reported to have a sensitivity ranging from 65% to 98% and a specificity of 72%–100%.^{13,14}

In this study, we applied an echo-planar MR imaging type of diffusion imaging with b-values of 0, 250, and 500 s/mm², which were sufficient to obtain high image quality and a high sensitivity for diagnosis of thyroid cancer. Diffusion-weighted MR imaging can be done with single shot or multi-shot. Diffusion-weighted single-shot multisection echo-planar imaging is characterized by a train of gradient echoes with a short echo image and a good signal intensity-to-noise ratio, but it may be associated with magnetic susceptibility artifacts. The diffusion-weighted fast spin-echo MR image is a multi-shot sequence characterized by multiple 180° refocusing pulses. It has a longer TE and a lower signal intensity-to-noise ratio than does the echo-planar sequence, without susceptibility artifacts.^{22,24–26} Wang et al,¹⁶ and Adel Razek et al,¹⁸ used an echo-planar type of diffusion-weighted MR imaging with b-values of 0, 500, and 1000 s/mm². Tezuka et al,²⁰ used a spin-echo type of diffusion-weighted MR imaging with b-values of 0.01, 128.01, and 288.02 s/mm² for characterization of diffusion of the thyroid gland.

There were a few limitations to the present study. First, the relatively small number (11.1%) of the malignant nodules limits the statistical power. This needs further study with a larger number of patients. Second, thyroid nodules <8 mm were not reported in this study. Improvement in the software of diffusion-weighted MR imaging may help in the detection of smaller lesions. Third, diffusion-weighted MR imaging is not conclusive as regards differentiation of thyroid cysts from hemorrhagic nodules, whose ADC values simulate those of malignancy; hence, diffusion-weighted MR imaging does not cancel the role of FNAB in sonographically diagnosed cystic thyroid nodules. Last, no internal standard of reference such as the CSF and/or spinal cord ADC was calculated.

Conclusion

We concluded that the ADC value is a new promising noninvasive imaging approach that can be used for characterization

of solitary thyroid nodules and differentiation between benign and malignant ones. Diffusion-weighted MR imaging does not help to differentiate among different types of malignant thyroid nodules but does reliably differentiate among various benign nodules. Further studies are needed to determine whether diffusion-weighted MR imaging could be added to the routine imaging technique used for differentiating malignant from benign solitary thyroid nodules.

References

1. Reading C, Charboneau W, Hay I, et al. **Sonography of thyroid nodules: a classic pattern diagnostic approach.** *Ultrasound Q* 2005;21:157–65
2. Weber A, Randolph G, Aksoy F. **The thyroid and parathyroid glands: CT and MR imaging and correlation with pathology and clinical findings.** *Radiol Clin North Am* 2000;38:1105–29
3. Tan G, Ghrib H, Reading C. **Solitary thyroid nodule: comparison between palpation and ultrasonography.** *Arch Intern Med* 1995;155:2418–23
4. Solbiati L, Osti V, Cova L, et al. **Ultrasound of thyroid, parathyroid glands and neck lymph nodes.** *Eur Radiol* 2001;11:2411–24. Epub 2001 Oct 25
5. Frates MC, Benson CB, Charboneau J, et al. **Management of thyroid nodules detected at US: Society of Radiologists in Ultrasound consensus conference statement.** *Radiology* 2005;237:794–800
6. Sahin M, Guvener N, Ozer F, et al. **Thyroid cancer in hyperthyroidism: incidence rate and value of ultrasound-guided fine-needle aspiration biopsy in this patient group.** *J Endocrinol Invest* 2005;28:815–18
7. Gooding G. **Sonography of the thyroid and parathyroid.** *Radiol Clin North Am* 1993;31:967–89
8. Bartolotta T, Midiri M, Galia M, et al. **Qualitative and quantitative evaluation of solitary thyroid nodules with contrast-enhanced ultrasound: initial results.** *Eur Radiol* 2006;16:2234–41
9. Yousem D. **Parathyroid and thyroid imaging.** *Neuroimaging Clin N Am* 1996;6:435–59
10. Gritzmman N, Koischwitz D, Retterbacher T. **Sonography of the thyroid and parathyroid glands.** *Radiol Clin North Am* 2000;38:1131–45
11. Papini E, Guglielmi R, Bianchini A, et al. **Risk of malignancy in nonpalpable thyroid nodules: predictive value of ultrasound and color-Doppler features.** *J Clin Endocrinol Metab* 2002;87:1941–46
12. Okamoto T, Yamashita T, Harasawa A. **Test performance of three diagnostic procedures in evaluating thyroid nodules: physical examination, ultrasonography and fine needle aspiration cytology.** *Endocr J* 1994;41:243–47
13. Gharib H, Goellner J. **Fine needle aspiration biopsy of thyroid: an appraisal.** *Ann Intern Med* 1993;118:282–89
14. Altavilla G, Pascale M, Nenci I. **Fine needle aspiration cytology of the thyroid gland diseases.** *Acta Cytol* 1990;34:251–56
15. Gotway M, Higgins C. **MR imaging of the thyroid and parathyroid glands.** *Magn Reson Imaging Clin N Am* 2000;8:163–82, ix
16. Wang J, Takashima S, Takayama F, et al. **Head and neck lesions characterization with diffusion-weighted echo-planar MR imaging.** *Radiology* 2001;220:621–30
17. Abdel Razek A, Kandeel A, Soliman N, et al. **Role of diffusion-weighted echo-planar MR imaging in differentiation of residual or recurrent head and neck tumors and posttreatment changes.** *AJNR Am J Neuroradiol* 2007;28:1146–52
18. Abdel Razek, Soliman N, Elkhannary S, et al. **Role of diffusion-weighted MR imaging in cervical lymphadenopathy.** *Eur Radiol* 2006;16:1468–77
19. Eida S, Sumi M, Sakihama N, et al. **Apparent diffusion coefficient mapping of salivary gland tumors: prediction of the benignancy and malignancy.** *AJNR Am J Neuroradiol* 2007;28:116–21
20. Tezuka M, Murata Y, Ishida R, et al. **MR imaging of the thyroid: correlation between apparent diffusion coefficient and thyroid gland scintigraphy.** *J Magn Reson Imaging* 2003;17:163–69
21. Thoeny H, Keyzer F. **Extracranial applications of diffusion-weighted magnetic resonance imaging.** *Eur Radiol* 2007;17:1385–93
22. Koh D, Collins D. **Diffusion-weighted MRI in the body: applications and challenges in oncology.** *AJR Am J Roentgenol* 2007;88:1622–35
23. Anderson J. **Tumours: general features, types and examples.** In: Anderson JR, ed. *Muir's Textbook of Pathology*. 13th ed. London: Edward Arnold; 1992:127–56
24. Bublulle F, Souillard R, Chechin D, et al. **Diffusion-weighted MR imaging sequence in the detection of postoperative recurrent cholesteatoma.** *Radiology* 2006;238:604–10
25. Baur A, Dietrich O, Reiser M. **Diffusion-weighted imaging of the spinal cord.** *Neuroimaging Clin N Am* 2002;12:147–52
26. Maeda M, Kato H, Sakuma H, et al. **Usefulness of the apparent diffusion coefficient in line scan diffusion-weighted imaging for distinguishing between squamous cell carcinomas and malignant lymphomas of the head and neck.** *AJNR Am J Neuroradiol* 2005;26:1186–92